HYDROLOGICAL PROCESSES
Hydrol. Process. **21**, 2823–2834 (2007)
Published online 21 December 2006 in Wiley InterScience
(www.interscience.wiley.com) DOI: 10.1002/hyp.6520

Influence of groundwater pumping on streamflow restoration following upstream dam removal†

Jim Constantz* and Hedeff Essaid
US Geological Survey, Menlo Park, CA 94025, USA

Abstract:

We compared streamflow in basins under the combined impacts of an upland dam and groundwater pumping withdrawals, by examining streamflow in the presence and absence of each impact. As a qualitative analysis, inter-watershed streamflow comparisons were performed for several rivers flowing into the east side of the Central Valley, CA. Results suggest that, in the absence of upland dams supporting large reservoirs, some reaches of these rivers might develop ephemeral streamflow in late summer. As a quantitative analysis, we conducted a series of streamflow/groundwater simulations (using MODFLOW-2000 plus the streamflow routing package, SFR1) for a representative hypothetical watershed, with an upland dam and groundwater pumping in the downstream basin, under humid, semi-arid, and arid conditions. As a result of including the impact of groundwater pumping, post-dam removal simulated streamflow was significantly less than natural streamflow. The model predicts extensive ephemeral conditions in the basin during September for both the arid and semi-arid cases. The model predicts continued perennial conditions in the humid case, but spatially weighted, average streamflow of only 71% of natural September streamflow, as a result of continued pumping after dam removal. Published in 2006 by John Wiley & Sons, Ltd.

KEY WORDS streamflow; dam removal; groundwater pumping; stream restoration

Received 27 July 2005; Accepted 2 June 2006

INTRODUCTION

Although dams often provide flood control, hydroelectric power, reliable reservoirs of surface water, and expansive recreational lakes, there is increasing interest in the potential advantages of accelerated dam removal. This is reflected in a steady stream of dam removal articles appearing in monthly scientific magazines (e.g. Francisco, 2004; Landers, 2004), as well as the popular press (e.g. Martin, 2004; McCool, 2004). The most pervasive negative downstream impacts of dams include degradation of the stream channel, riparian zone, and biota habitats due to lower peak streamflow (e.g. Graf, 1980; Williams and Wolman, 1984; Ligon *et al*., 1995; Collier *et al*., 1996; Pohl, 2003), as well as risks associated with dam failure (e.g. Thomas, 1976; Petroski, 2003). Thus, removal of dams is often perceived as a means of restoring natural streamflow and sediment transport, resulting in improved riparian corridors, fishery habitats, sports fishing, recreational rafting, and reappearance of a more pastoral, riparian setting. However, removal of a specific dam not only eliminates the intended benefits of the dam, but also induces cumulative liabilities related to removal of the dam, such as dispersal of accumulated sediment (e.g. Shuman, 1995). Regardless of the pros and cons associated with 'the dam dilemma', the issue has been universally viewed as a surface phenomenon, involving surface-water hydraulics, sediment transport, fishery, benthic, and riparian ecology, as well as a plethora of aesthetic issues. As suggested by Constantz (2003), this vantage point possesses merit, but neglects the influence of groundwater pumping on post-dam removal streamflow, especially during the low-flow season.

We analyse the combined impact of an upland dam and groundwater pumping in the basin on streamflow for the natural case (before the presences of both dam and pumping), for the case with a dam impounding a large reservoir without pumping in the basin, for the case with a dam and with pumping in the basin, and finally for the case after dam removal and with continued pumping in the basin. We evaluate the influence of groundwater pumping on basin streamflow for each case under humid, semi-arid and arid conditions, where precipitation predominantly occurs in the winter months, resulting in relatively dry summer conditions (the precipitation condition under which a large dam is commonly erected). We initiate our research with the semi-arid climate conditions and examine streamflow before, during, and after the presence of an upland dam, and then expand our investigation to include the humid and arid conditions.

CONCEPTUAL FRAMEWORK

As discussed in speculative work (Constantz, 2003), Figure 1 provides an idealized sequence of four scenarios depicting a conceptual hydrogeologic cross-section through a semi-arid watershed spanning hundreds of kilometres from upland mountainous terrain draining toward

* Correspondence to: Jim Constantz, US Geological Survey, Building 15 McKelvey Building, 345 Midlefield Road, Menlo Park, CA 94025, USA. E-mail: jconstan@usgs.gov

a groundwater basin, with a major stream system flowing out of the mountains. The upper panel in the figure depicts a natural setting, where the water table approaches ground surface as the stream discharges from the mountainous bedrock. The idealized streamflow shown in the panel is representative of long-term average hydrograph records for large, semi-arid watersheds throughout the western USA, characterized by high peak flow during the wet season and prolonged base flow due to groundwater discharge during the dry season. The second panel depicts the general changes in the hydrologic system after the erection of a dam, resulting in creation of a large reservoir on the flank of the mountainous terrain. The hydrograph inset in the panel shows the moderating effects of the dam on the streamflow, such that the dam buffers spring peak flow and summer low flow is enhanced by dam releases of the stored portion of the peak flow. The third panel depicts the general change in the hydrologic system after groundwater pumping withdrawals have drawn down the water table well below the elevation of the streambed. If stream losses are insufficient to maintain full saturation of streambed-sediments, the water table declines below the elevation of the streambed. Once air enters draining streambed sediments, streamflow loss is determined by gravity drainage (i.e., unit hydraulic gradient times streambed hydraulic conductance), and the loss is usually independent of the elevation of the water table. The hydrograph inset in this panel shows a significant decrease in streamflow at the downstream hydrograph, due to streamflow losses caused by the lowered water table; however, dam releases are large enough to sustain down-channel streamflow. The fourth panel depicts the general change in the hydrologic system after dam removal with continued groundwater pumping. In addition to dispersal of decades of accumulated sediment trapped behind the dam, one probable outcome of removal is a hydrograph characterized by a return to large peak flow in the wet season followed by prolonged low flow during the dry season. Peak streamflow is likely to resemble the natural peak flow, if the watershed upstream of the previous dam location is still in its natural state. In contrast, post-dam low streamflow may be greatly reduced relative to natural low flow, due to antecedent groundwater pumping conditions creating a higher streamflow loss environment than was present under natural conditions. Without the summer dam releases enhancing streamflow there is a real potential for no-flow conditions in the stream as the dry season progresses. This scenario warrants attention, due to the clear impact of no-flow conditions on fish and riparian habitats, as well as recreational and aesthetic resources. Thus, it has long been appreciated that a dam supporting a large reservoir functions as a hydrologic 'safety valve' to moderate streamflow, but we contend that, due to basin groundwater pumping, in many settings the presence of the dam has become mandatory for maintaining summer streamflow in the basin.

We apply a pair of approaches suggested in an earlier volume of this journal (Constantz, 2003), to test this prediction of decreased streamflow following upland dam removal. First, we conduct qualitative inter-watershed comparisons for watersheds currently including various combinations of dam and pumping stresses. Specifically, we perform a qualitative comparison of hydrographs for semi-arid watersheds with streams emanating from the western foothills of the Sierra Nevada Mountain Range flowing west into the Central Valley, CA. In the present study, this comparison is developed as a reference frame for a quantitative analysis of streamflow in humid, semi-arid, and arid watersheds with dam and pumping stresses. We quantitatively predict streamflow in a generic watershed with model simulations mimicking the four scenarios depicted in Figure 1. The quantitative analysis is accomplished using the groundwater flow model MODFLOW-2000 (Harbaugh *et al*., 2000), with the streamflow routing package SFR1 (Prudic *et al*., 2004). The suite of MODFLOW programs has been extensively tested worldwide and has been found to represent Darcian groundwater flow correctly, as well as associated hydrological processes, including stream exchanges with groundwater. Preliminary analysis of watersheds and initial MODFLOW-2000 plus SFR1 generation of simulated streamflow both produced intriguing results (Constantz and Essaid, 2004), which warrant expanded investigation. Here, we report on a comprehensive expansion of this approach to construct a concise set of trends over a range of humid to arid conditions.

QUALITATIVE WATERSHED COMPARISONS

A summary of the qualitative inter-watershed comparison is assembled in Figure 2. The figure displays average monthly streamflow hydrographs for five streams in a portion of the Central Valley residing in the semi-arid Sacramento Valley and the drier San Joaquin Valley. In the upper portion of the figure, mean monthly hydrographs are graphed for the Bear, Cosumnes, and Mokelumne Rivers. The Bear River has a dam with a small reservoir (storage capacity is $0{\cdot}05 \times 10^6$ acre-feet, or $6{\cdot}2 \times 10^7$ m^3) in its upland reaches, and the Mokelumne River has several dams with large reservoirs in its upland reaches (cumulative storage capacity is $\sim 0{\cdot}75 \times 10^6$ acre-feet, or $9{\cdot}3 \times 10^8$ m^3). The Cosumnes River basin is the sole watershed without a dam emanating from west side of the Sierra Nevada Range. Groundwater has been a significant source of water in the Central Valley since pumping began in 1880 (Bertoldi *et al*., 1991), and all three watersheds are stressed by depleted groundwater conditions due to extensive groundwater pumping in their lower basins. The different dam conditions in the basins result in visibly different temporal patterns in streamflow hydrographs. The Bear and Mokelumne hydrographs are analogous to the third panel in Figure 1. Dry-season dam releases sustain streamflow

Published in 2006 by John Wiley & Sons, Ltd.

DOI: 10.1002/hyp

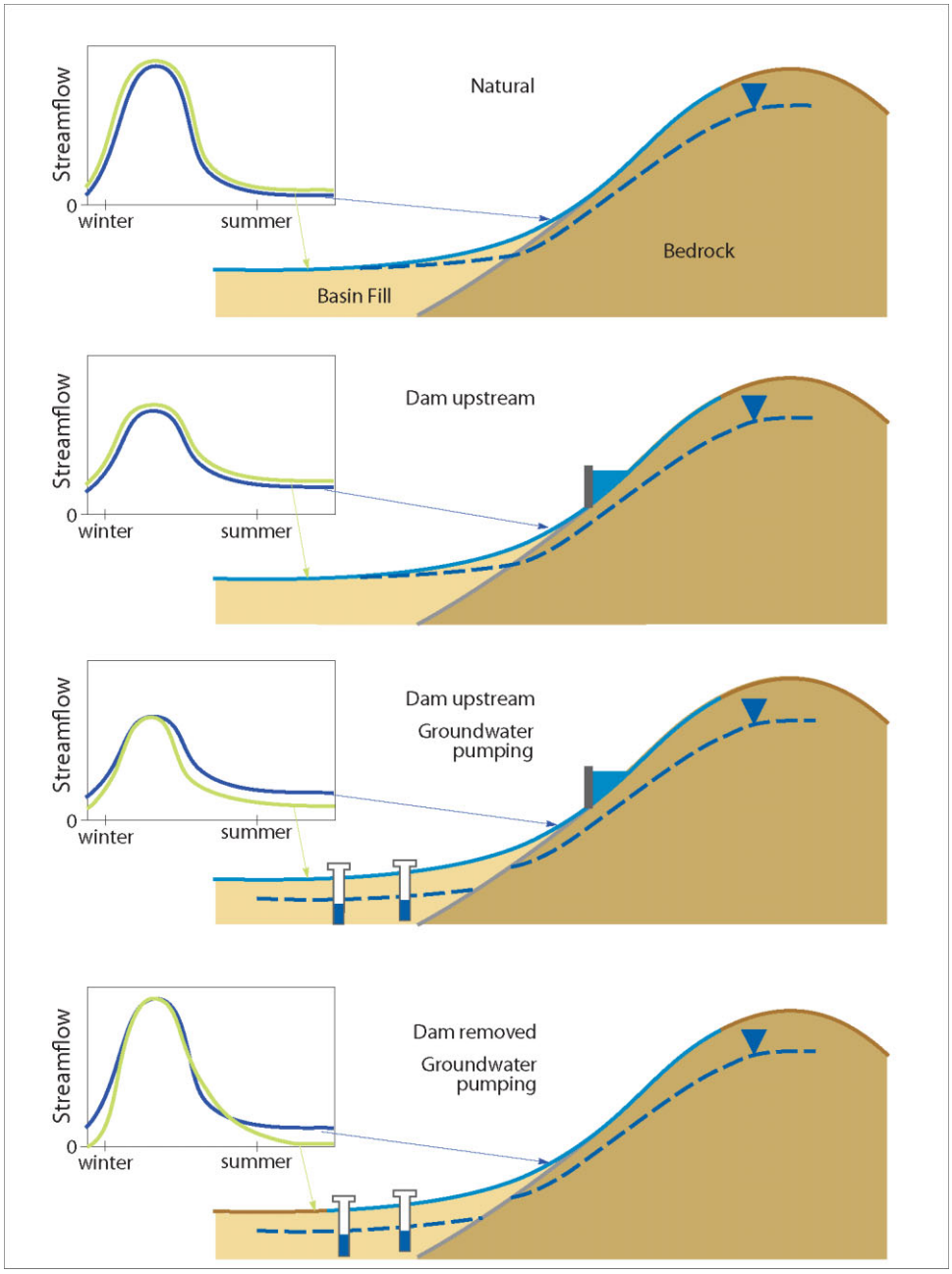

Figure 1. Four conceptual hydrogeologic cross-sections and corresponding hydrographs showing a stream draining from mountainous terrain into a large alluvial basin, for the cases of: (1) a natural setting without large reservoirs or groundwater pumping (i.e. withdrawals); (2) a dam creating a large reservoir at the base of the mountainous terrain; (3) a dam and pumping in the alluvial basin; (4) removal of the dam and continued pumping (modified from Constantz (2003))

with the differential in reservoir capacity explaining the disparity in late-summer streamflow. The hydrograph for the undammed Cosumnes River, analogous to the fourth panel in Figure 1, shows vanishing streamflow in the late summer months.

This inter-watershed comparison suggests that dam removal on the Bear or Mokelumne Rivers might lead to ephemeral or intermittent streamflow conditions, qualitatively similar to the long-term average monthly streamflow logged for the Cosumnes River. In the lower portion of Figure 2, a similar pattern is evident in hydrographs for the Calaveras and Stanislaus Rivers. New Hogan Dam (storage capacity is $0{\cdot}3 \times 10^6$ acre-feet, or $3{\cdot}7 \times 10^8$ m^3) went into operation on the Calaveras River in 1964, and New Melones Dam (storage capacity is $2{\cdot}4 \times 10^6$ acre-feet, or $3{\cdot}0 \times 10^9$ m^3) went into operation on the Stanislaus River in 1983, significantly enhancing summer streamflow. These inter-watershed comparisons confirm that there is a clear positive correlation between reservoir storage capacity and minimum mean monthly summer streamflow for these extensively developed groundwater basins. The Calaveras River pre-dam compared with present conditions presents an interesting third case, in which pre-dam streamflow was ephemeral for negligible groundwater pumping, whereas the river today is perennial because of dam releases.

Published in 2006 by John Wiley & Sons, Ltd.

DOI: 10.1002/hyp

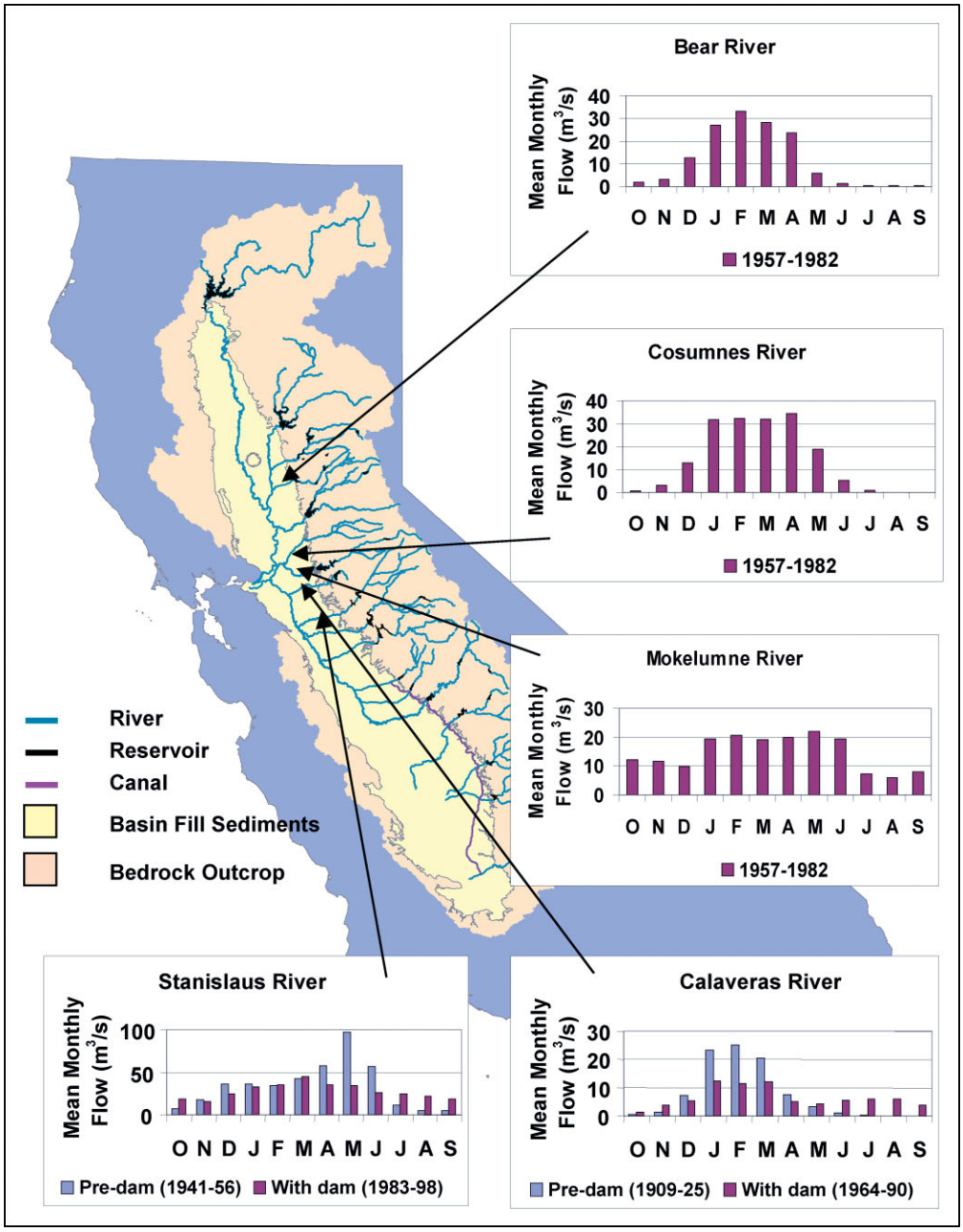

Figure 2. The middle portion of the Central Valley (CA) is shown, with monthly streamflow hydrographs for the rivers indicated. Streamflow records before construction of the dam and with the dam are noted as separate bar graphs, where available

In summary, qualitative comparison of observed monthly average streamflow trends for watersheds representing the conceptual scenarios depicted in Figure 1 supports the hypothesis that, when dams are removed in developed groundwater basins, baseflow may be greatly reduced relative to natural baseflow as a result of lower water table elevations in the developed basin relative to the natural setting. Also, there is increased potential for periods without streamflow, as a consequence of pumping-induced depleted groundwater conditions in the lower watershed. In addition, some rivers that flow all year may revert to their natural ephemeral state. In the following sections we illustrate these interactions by simulating groundwater and surface-water flow in a relatively simple, yet realistic hypothetical watershed.

QUANTITATIVE WATERSHED SIMULATIONS

Numerical modelling of a generic watershed is used to illustrate and quantify the effects of groundwater pumping and dams on streamflow. The model is designed to reproduce regional changes in the watershed and relative changes in streamflow as the watershed goes from the natural state to developed conditions. The simulations do not represent an actual watershed; however, model geometry, parameters, and stresses were chosen to be realistic for typical watersheds in the western USA while still maintaining simplicity of model formulation.

Model approach

The modular finite-difference three-dimensional groundwater flow model MODFLOW-2000, with the

SFR1 stream–aquifer interaction and streamflow-routing package and the grid-block rewetting options, was used to simulate monthly streamflow in a generic watershed for the four general scenarios shown in Figure 1. Model input set-up was facilitated by use of the MODFLOW GUI, version 4 (Winston, 2000). The SFR1 package required that the stream be discretized into a network of stream reaches, with each reach associated with a particular finite-difference grid block. Properties of the reach include the width, thickness, and hydraulic conductivity of streambed sediments, as well as the depth of water in the stream. Complex cross-section geometries can be represented using SFR1, and depth and width can be calculated as a function of flow rate. The stream package SFR1 computes the exchange of water between the stream and aquifer using Darcy's law. Flow is routed through the network of stream reaches assuming streamflow is steady and uniform for each time step period, such that each reach's volumetric inflow rate is equal to the outflow rate. No water is added to or removed from storage in the surface channels. Delay in water or solute transport from an upstream reach to a downstream reach is caused by exchanges with groundwater. SFR1 is designed for modelling long-term changes (months to hundreds of years) in average flow. The SFR1 approach is not recommended for modelling the transient exchange of water between stream reaches and shallow groundwater when the objective is to examine short-term effects (minutes to days) caused by rapidly changing streamflow. Another limitation of the SFR1 approach is that leakage through the streambed is transmitted to the water table without delay. This may not be reasonable when the head in the aquifer is below the bottom elevation of the streambed, such as for intermittent or ephemeral channels where the water table is tens to hundreds of metres below the streambed. However, in our application of the SFR1 package we focus on average monthly streamflow rather than short-term streamflow in response to storms. Also, the water table is generally connected to the stream except in the dry parts of the stream channel, where there would be no flow through the streambed. Therefore, the assumptions of the SFR1 package are acceptable for this analysis.

We used MODFLOW-2000 with SFR1 first to simulate streamflow for semi-arid natural conditions (scenario 1 in Figure 1), then introduced a dam (scenario 2), added pumping (scenario 3), and finally removed the dam leaving pumping in place (scenario 4). To examine the influence of climate on streamflow we repeated the simulations for more humid conditions (two times the groundwater recharge of the base case), and more arid conditions (one-half the groundwater recharge of the base case). Our approach for simulating streamflow using the groundwater model assumes that average monthly streamflow predominantly reflects rapid shallow (interflow) and slow deep (baseflow) groundwater contributions (Kirchner *et al*., 2000; Uhlenbrook *et al*., 2002) that can be reproduced by applying monthly diffuse recharge (precipitation minus evapotranspiration) over the model area. This approach neglects short-lived event contributions to streamflow, such as overland flow.

Model framework

The geometry and properties of the simulated generic watershed are loosely based on the general characteristics of watersheds in the Central Valley, CA (Bertoldi *et al*., 1991; Gronberg *et al*., 1998). The domain of the model extends from the upland bedrock headwaters of a stream down to the sediment-filled basin axis (Figure 3) and is 180 km long, 15 km wide and 1·3 km deep, including a stream with a potential length of 180 km. In the upper reaches, the stream is divided into north, south, and main stems with their confluence upstream of a dam situated in the domain above the bedrock–basin-fill contact. Simulated streamflow is an outcome of the model solution; no initial streamflow is imposed. Because of the regional scale of the model, discretization is somewhat coarse in order to facilitate practical simulation times. Horizontal discretization is 1000 m in the direction parallel to the stream (184 columns). Perpendicular to the stream, where we expect steeper gradients, the discretization varies from 200 m adjacent to the stream to 600 m away from the stream (33 rows). Vertical discretization increases from 50 m for the top layer to 300 m for the bottom layer (10 layers). This level of discretization allowed us to examine the regional response of the watershed to large-scale changes in climate and dam presence/absence.

The basin sediments were assigned properties of silty sand (horizontal hydraulic conductivity $K_h = 1 \times 10^{-4}$ m s^{-1}; vertical hydraulic conductivity $K_z = 1 \times 10^{-5}$ m s^{-1}; specific yield: 0·05 (Freeze and Cherry, 1979)). As depicted in Figure 3, bedrock had a depth-dependent hydraulic conductivity (Manning and Ingebritsen, 1999), adjusted at shallow depths for properties of unconsolidated material, and a specific yield of 0·003.

The flux of water through the streambed q_{sb} is given by Darcy's law (Prudic *et al*., 2004):

$$q_{sb} = -K_{sb}\frac{H_s - H_g}{b_{sb}}w_{sb} \quad (1)$$

where K_{sb} is the streambed hydraulic conductivity, b_{sb} is the streambed thickness, H_s is the hydraulic head in the stream (stream stage), H_g is the hydraulic head in the groundwater, and w_{sb} is the stream width. In a typical watershed the properties of the streambed will vary along the length of the stream. For example, stream width might increase downstream as discharge increases, and conductivity might decrease downstream as bed sediments become finer. To maintain model simplicity, we assumed that the net resistance to flow through the streambed sediments ($K_{sb}w_{sb}/b_{sb}$) was constant by assigning streambed sediments a hydraulic conductivity of 1×10^{-4} m s^{-1}, a constant width of 1 m, and constant thickness of 1 m. Early simulations showed that changes in streambed properties had little effect on streamflow response, because small adjustments in groundwater

Published in 2006 by John Wiley & Sons, Ltd.

DOI: 10.1002/hyp

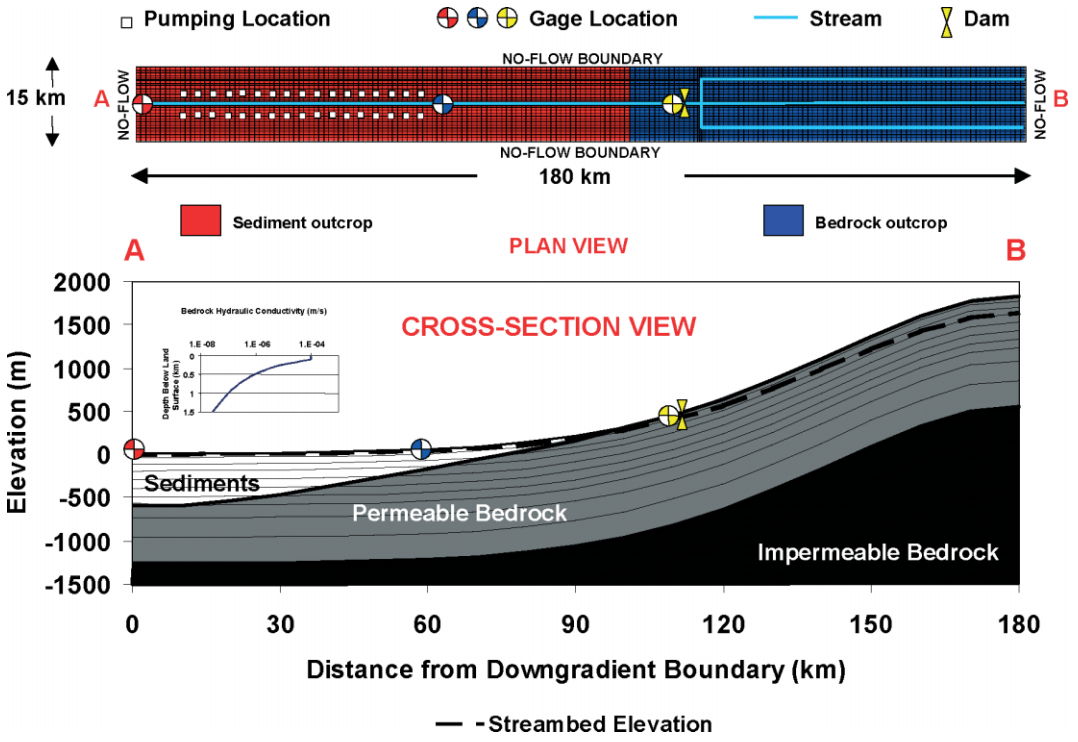

Figure 3. The upper schematic is a plan view showing the model geometry, boundaries, discretization, and stream network divided into north, south, and main stems, with their confluence upstream of a dam situated above the bedrock–basin-fill contact. The lower schematic is model domain portrayed as a cross-section in a similar aspect as Figure 1

levels (relative to the relief in the basin) were sufficient to compensate for increased or decreased resistance to flow in the streambed. To help reduce model non-linearity and avoid numerical instability, we assumed a constant depth of water in the stream, and the stream stage H_s was set to the elevation of the streambed plus 1 m. However, when H_g dropped below H_s, loss of water from the stream only occurred when sufficient surface water flow from upstream was available.

No-flow conditions were assigned to the side and bottom boundaries of the model. The downstream boundary represents the symmetry boundary that develops in the common hydrological setting where tributaries flow into a main river from highlands on both sides of the basin. To examine the effect of the no-flow assumption on the downstream boundary, we ran the semi-arid base case simulation with the left side boundary set as a river flowing perpendicular to the stream. Substituting the river for the no-flow downstream boundary produced a small decrease in streamflow near the confluence with the river, because some groundwater discharged to the river at the boundary rather than to the stream. For example, in the semi-arid watershed, October streamflow at the boundary was reduced by only $2 \cdot 6\%$ from $7{\cdot}33$ m^3 s^{-1} to $7{\cdot}14$ m^3 s^{-1}. Consequently, for simplicity, a no-flow boundary was employed rather than a main stem river boundary on this boundary of the simulation model.

Model fluxes

Water can enter and exit the watershed across the top land-surface boundary. Water enters the system as spatially and temporally distributed recharge. Water can leave the system as streamflow, evapotranspiration, and groundwater pumping withdrawals. Recharge occurs during the wet season when precipitation P is greater than potential evapotranspiration PET. The spatial and temporal distributions of recharge specified in the model scenarios were abstracted from observations of long-term average monthly precipitation (National Oceanic and Atmospheric Administration, 2002) and potential evapotranspiration (California Irrigation Management Information System, 1999) patterns for the Willamette Valley (OR), Sacramento Valley (CA), and San Joaquin Valley (CA), representing examples of humid, semi-arid, and arid basins respectively. During the dry season, some water leaves the groundwater in the watershed through evapotranspiration ET from shallow water table zones. The magnitude and duration of annual wet-season recharge (the sum of $(P - \text{PET})$ for months with $P >$ PET) is a function of land surface elevation and climate. Recharge increases with elevation, as illustrated by the data shown in Figure 4a for four stations with increasing elevation. Figure 5a illustrates the elevation-dependent longitudinal distribution of annual wet-season recharge applied in the simulations. The total wet-season recharge applied in the simulations for the more humid case (average 54 cm year^{-1}) was twice that of the semi-arid base case (average 27 cm year^{-1}), and the wet-season recharge for the more arid case (average $13{\cdot}5$ cm year^{-1}) was half that of the semi-arid (base) case.

Observation of monthly $(P - \text{PET})$ values for locations with similar altitudes but different climates showed that the length of the recharge season (months for which

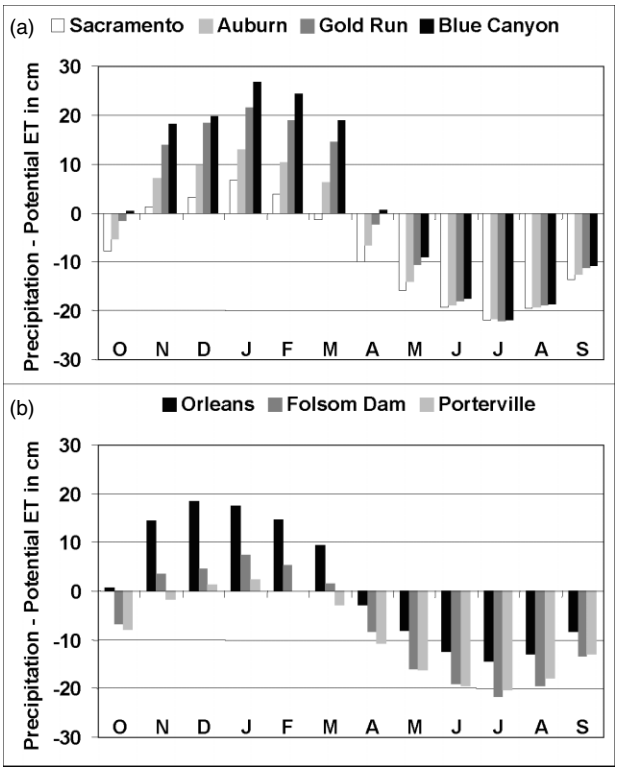

Figure 4. Climate data used to formulate model recharge and evapotranspiration ET estimates. (a) Precipitation minus PET at four stations with increasing elevation: Sacramento (CA), 12 m a.s.l., 38°33′N, 121°25′W; Auburn (CA), 414 m a.s.l., 38°54′N, 121°05′W; Gold Run (CA), 1012 m a.s.l., 39°09′N, 120°51′W; Blue Canyon (CA), 1609 m a.s.l., 39°17′N, 120°43′W. (b) Precipitation minus PET at three stations with similar elevation but different climate: Orleans (CA), 128 m a.s.l., 41°18′N, 123°32′W, relatively humid; Folsom Dam (CA), 106 m a.s.l., 38°42′N, 121°10′W, semi-arid; Porterville (CA), 120 m a.s.l., 36°04′N, 1119°01′W, relatively arid

$P >$ PET) was a function of climate (Figure 4b), with the recharge season being shorter in more arid climates. Generally, the recharge seasons corresponded to October through to April (7 months), November through to March (5 months), and December through to February (3 months) for the humid, semi-arid, and arid climates respectively. This monthly temporal distribution of recharge was represented in the model by multiplying annual wet-season recharge at each grid block (Figure 5a) by the monthly factors shown in Figure 5b.

During the dry season (when there is no natural recharge), water may leave the system through evapotranspiration from shallow groundwater. To simplify comparison of model results, we have kept total dry-season actual evapotranspiration ET constant (6·75 cm year^{-1}) for all climates and elevations. We assume that increased evaporative demand (PET) generally coincides with decreased vegetation and water availability, causing dry-season ET to be less sensitive to climate and elevation than PET. Model input dry-season monthly evapotranspiration was obtained by multiplying annual dry-season ET by the monthly factors shown in Figure 5c. Dry-season evapotranspiration represented 12·5%, 25% and 50% of annual recharge for the humid, semi-arid, and arid cases respectively.

The net annual recharge distribution (wet-season recharge minus dry-season ET) is shown by the dashed lines in Figure 5a. At the lower elevations, for both the semi-arid and arid cases, the net annual recharge is negative because dry-season ET is greater than wet-season recharge, resulting in a net loss of groundwater. Figure 5e shows the spatial average of the resulting net monthly recharge function for each climate case and illustrates the differences in recharge amount and duration for the humid, semi-arid, and arid climate simulations.

The presence of a dam temporally redistributes streamflow throughout the year. Examination of daily inflow to and outflow from Lake McClure (a reservoir formed by New Exchequer Dam on the Merced River, CA) showed that total outflow for the period from 1995–1999 was 98% of the inflow. Therefore, for simplicity and ease of comparison across scenarios, we have assumed that cumulative annual discharge below the dam site is equivalent to annual discharge for scenarios without the dam in place. Because of the regional nature of the analysis, potential influences in the immediate vicinity of the dam site, such as localized recharge beneath the reservoir and localized increases in evaporation due to the reservoir, are not included in this model. Reservoir flow releases for simulations with a dam were obtained by multiplying the annual simulated streamflow at the dam location, obtained from the natural conditions scenario simulation, by the multiplication factors shown in Figure 5d. This produced simulated releases that followed a pattern similar to the seasonal distribution of releases observed for regulated streams such as the Calaveras River shown in Figure 2. These release flow rates were then introduced into the first stream segment downgradient from the dam site in the model (upper gauge in Figure 3). The actual reservoir was not simulated because the local effects of the reservoir on groundwater flow are small (assuming a relatively non-leaky reservoir) compared with the scale of the watershed.

To simplify comparisons, the amount of total annual pumpage ($1{\cdot}5 \times 10^8$ m^3) in simulations with pumping was similar for each climate case. This amount of pumpage corresponds to an annual depth of water of 16·7 cm over the lower 60 km of the basin. This is a relatively small fraction of the annual water deficits estimated for Orleans, CA (59 cm), Loomis, CA (105 cm), and Porterville, CA (110 cm) by summing the monthly deficits shown in Figure 4b caused by PET being greater than P. Annual pumpage was distributed over the dry months, using the same monthly multiplication factors used for ET (Figure 5c), because it was assumed that groundwater was the primary source of irrigation water and that irrigation demands corresponded to ET. The net result was that pumpage represented 10%, 20%, and 40% of annual recharge for the humid, semi-arid, and arid cases respectively.

To maintain simplicity of this illustrative analysis, the simulations did not include the effects of irrigation return flow, the effects of surface water diversion for irrigation, or snowmelt dynamics. Irrigation return flow would tend

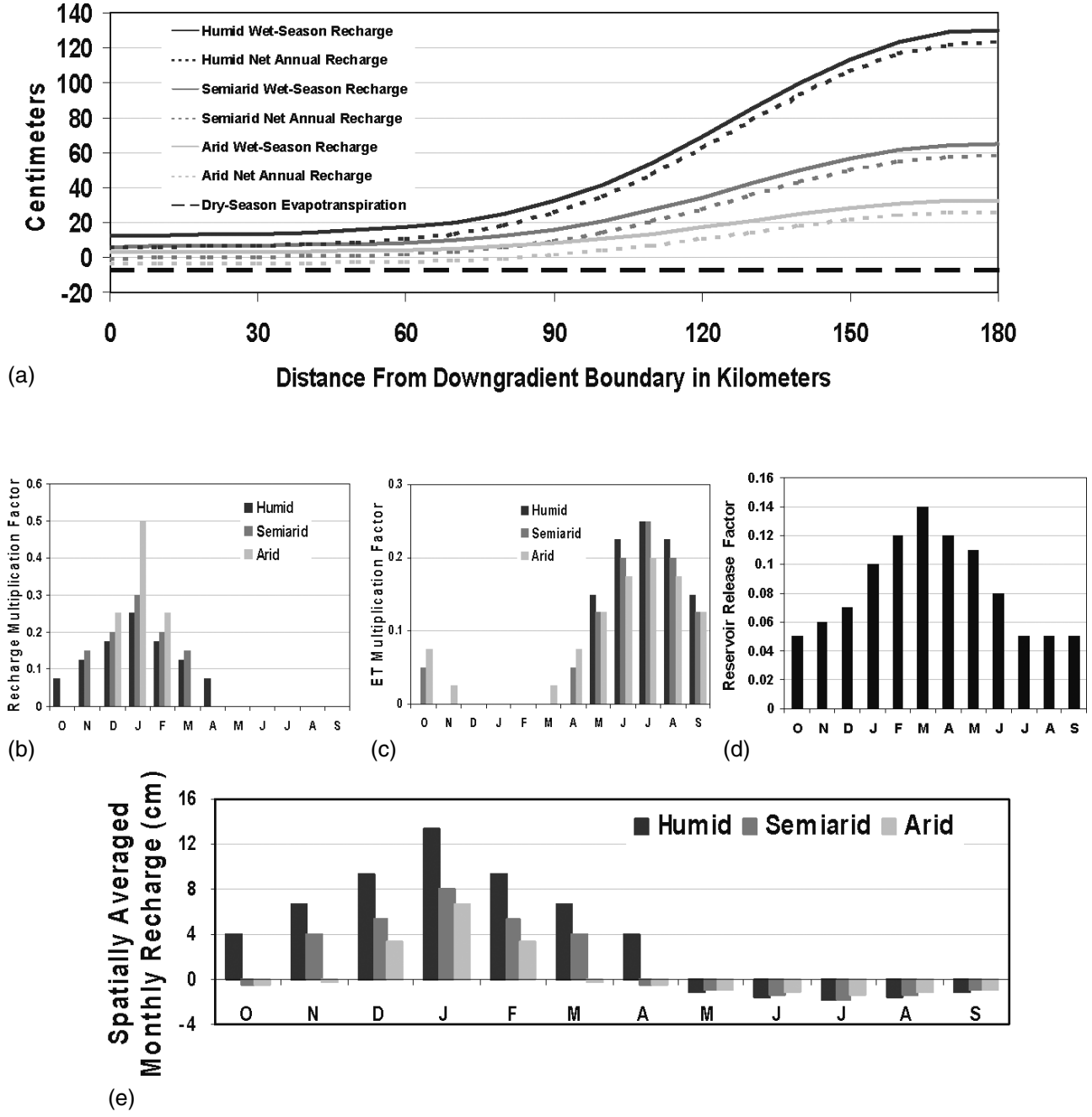

Figure 5. Graphs showing the model: (a) longitudinal distribution of annual recharge, with the dam site at 110 km upstream of the axis of the basin; (b) monthly recharge multiplication factor; (c) ET multiplication factor; (d) reservoir release factor; (e) spatially weighted average monthly recharge. Recharge input functions are for arid, semi-arid, and humid conditions with dry summers; and for each climate case, the total annual pumpage and total dry-season evapotranspiration are equal

to enhance summer streamflow; however, surface water diversions would significantly decrease streamflow. The dynamics of snowmelt, which is climate dependent and highly variable from year to year, would alter the timing of peak wet-season streamflow.

Model results and discussion

The model was run for 60 months, with stress periods of 1-month duration, to simulate each of the four scenarios detailed in Figure 1 for all three climate cases. After the 5-year simulation period, each case reached a quasi-steady state such that net annual applied recharge approximately equalled the simulated total annual discharge to the stream, with the final year of simulated streamflow reported here. The groundwater heads obtained at the end of the natural conditions simulations were used as the initial conditions for the subsequent simulated cases. Figure 6 provides 12 hydrographs of simulated monthly streamflow at the end of each monthly stress period for the four scenarios, under humid (Figure 6a), semi-arid (Figure 6b), and arid (Figure 6c) conditions. In the figure, the bar graphs represent monthly streamflow at 1, 50, and

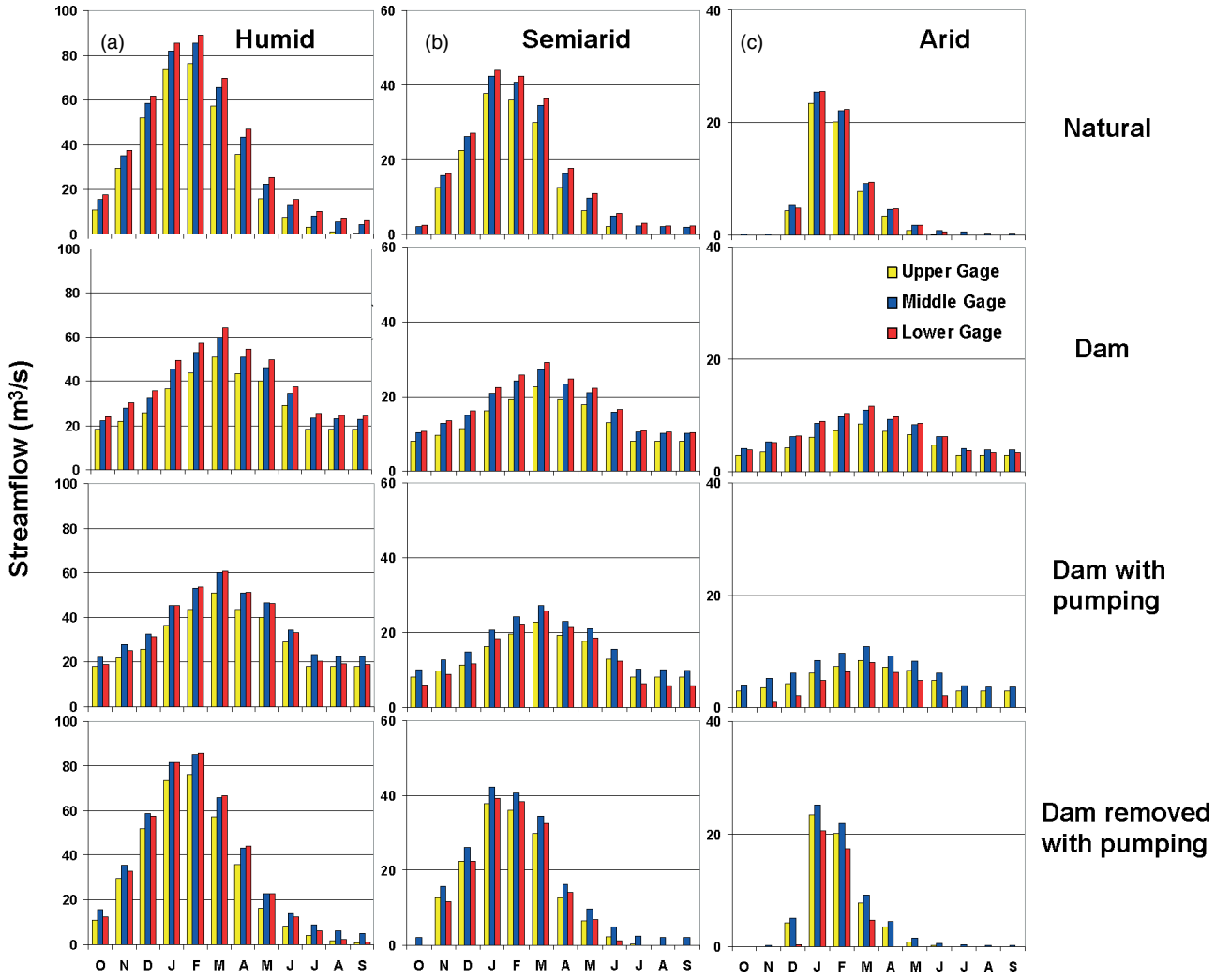

Figure 6. Model-predicted hydrographs at the three gauges obtained over the water year of 5-year simulations for (a) the humid conditions, (b) semi-arid conditions, and (c) arid conditions as described in the text. The light-, dark-, and medium-shaded bar graphs represent mean monthly streamflow at the upper, middle, and lower streamgauges, which are located at 1 km, 60 km, and 110 km from the dam spillway respectively

110 km below the dam site. Comparison of the simulated semi-arid hydrographs (Figure 6b) with Figures 1 and 2 shows consistent qualitative agreement between simulated, predicted, and measured streamflow. Simulation results depict reductions in late-summer streamflow for all three cases after dam removal, with significant increases in the duration of no-flow periods in reaches for the semi-arid and arid cases. Examining the nature of seasonal low flow in the simulated scenarios provides a basis for considering potential impacts of dam removal, and subsequent reduced summer streamflow on stream water quality, biological indices, and recreational value of reaches below existing dams.

Spatially weighted average September streamflow was obtained for each simulated case by averaging the flows from all 110 of the 1 km long model segments comprising the entire stream channel below the dam. Table I provides simulated average September streamflow, as well as September streamflow at the streamgauge 110 km below the dam, expressed in absolute magnitude and as a percentage of natural September streamflow. The streamflow values at this gauge are featured in Table I, because the influence of groundwater conditions creates the greatest impact on streamflow at this location in the basin. In addition, Table I provides the percentage of the 110 km channel below the dam sustaining September streamflow for each of the 12 scenarios. To obtain a sense of the impact of dam removal relative to current conditions, we can compare simulation results for the dam with pumping versus simulation results for the dam removed with pumping. For example, under the same precipitation and recharge model functions, September streamflow averaged over the entire 110 km reach is predicted to be many times greater than September streamflow without the dam. Also note that, after dam removal, the September streamflow at the 110 km gauge is predicted to be only 6% of pre-dam removal flow for the humid case, and the channel is predicted to run dry for the semi-arid case. Finally, for the arid case, September streamflow at the 110 km gauge is predicted to be absent due to groundwater pumping with or without a dam present upstream. The last column in Table I gives predictions of the portion of the stream channel containing streamflow during September for each of the 12 conditions. One can observe

Table I. September flow along stream channel below dam

Scenario	Spatially weighted average flow for entire 110 km channel		Flow at the 110 km gauge (gauge 110 km below dam)		Percentage of channel with flow (%)
	$m^3\ s^{-1}$	Percent of natural flow (%)	$m^3\ s^{-1}$	Percent of natural flow	
Humid conditions					
Natural	4·14	100	6·18	100	100
Dam	22·2	536	24·4	395	100
Dam with pumping	20·4	493	18·8	304	100
Dam removed with pumping	2·94	71	1·18	19	100
Semi-arid conditions					
Natural	1·74	100	2·35	100	100
Dam	9·77	561	10·4	443	100
Dam with pumping	8·36	480	5·80	247	100
Dam removed with pumping	0·746	43	0	0	68
Arid conditions					
Natural	0·167	100	0·193	100	68
Dam	3·54	2120	3·38	1751	100
Dam with pumping	2·37	1419	0	0	88
Dam removed with pumping	0·109	6	0	0	40

that the September channel becomes progressively drier through each of the four cases under humid, semi-arid, and arid environments. Figure 7, discussed below, provides an expanded portrayal of the hydrologic state of the channel under each condition.

Figure 7 displays graphs of simulated streamflow patterns below the dam site for May and September under humid, semi-arid, and arid conditions. Comparisons between each graph portray significant differences in the spatial patterns of streamflow for each scenario in the humid, semi-arid, and arid watersheds. Using May as an example, the semi-arid graph under natural conditions indicates that the stream is gaining and streamflow discharge at the dam site is about 5 $m^3\ s^{-1}$, increasing to about 7 or 8 $m^3\ s^{-1}$ in the reach 45 to 60 km below the dam site, and increasing to about 10 $m^3\ s^{-1}$ at the basin axis 110 km below the dam site. As an example for September, the arid graph for the dam with pumping scenario indicates that the stream transitions from gaining to losing and releases from the dam are about 3 $m^3\ s^{-1}$, increasing to about 4 $m^3\ s^{-1}$ in the channel 50 km below the dam site, and dissipating to no-flow conditions at 95 km below the dam site. Inspection of each graph confirms the dominant influence of the dam in upstream sections of the channel and the importance of groundwater pumping in the downstream sections of the channel, except for the humid case during May where groundwater discharge overwhelms pumping during that season. Of considerable relevance to the issue of dams and groundwater is the semi-arid graph for September. Under natural conditions, simulated streamflow travels the entire length of the channel to the axis of the groundwater basin (contributing streamflow to main stem river flowing along the axis), whereas streamflow ceases well up the stream channel from the axis of the groundwater basin for post-dam conditions with groundwater pumping. This would suggest that dam removal on tributaries may contribute to reduction of streamflow on main stem rivers, if groundwater discharge fails to replace streamflow substantially.

Simulation results suggest that humid watersheds may be less severely impacted by dam removal (scenario 4) than the drier watersheds. Though streamflow is predicted to decrease to as low as 19% of natural flow at the 110 km gauge, the channel remains flowing under the imposed groundwater pumping at 10% of annual recharge. Simulation results illustrate that semi-arid watersheds may not be capable of supporting streamflow following dam removal for watersheds that supported perennial flow under natural conditions. Though streamflow is naturally ephemeral for arid watersheds, simulation results indicate that the extent and duration of dry-channel conditions increases following dam removal. For both the semi-arid and arid watersheds, the extent and duration of dry-channel conditions following dam removal are a result of lower groundwater levels, potentially leading to both ecological and economic impacts in the basin. Finally, inspection of simulation results portrayed in Figure 7 suggests the possibility that some currently perennial streams with upstream dams were naturally ephemeral, indicating that natural groundwater conditions were incapable of sustaining lower basin summer streamflow even before groundwater pumping. As shown in Figure 2, the pre-dam and dam hydrographs displayed for the Calaveras River support this implication.

We explored a hypothetical case beyond scenario 4 in Figure 1 (removal of the dam) in which groundwater pumping withdrawals ceased following dam removal. As discussed earlier, cessation of pumping after loss of a primary reservoir would be exceptional and, therefore, was not included in the list of scenarios analysed in depth. However, in theory, a conservation district or stream-restoration foundation could purchase all groundwater rights in a basin during the course of dam removal,

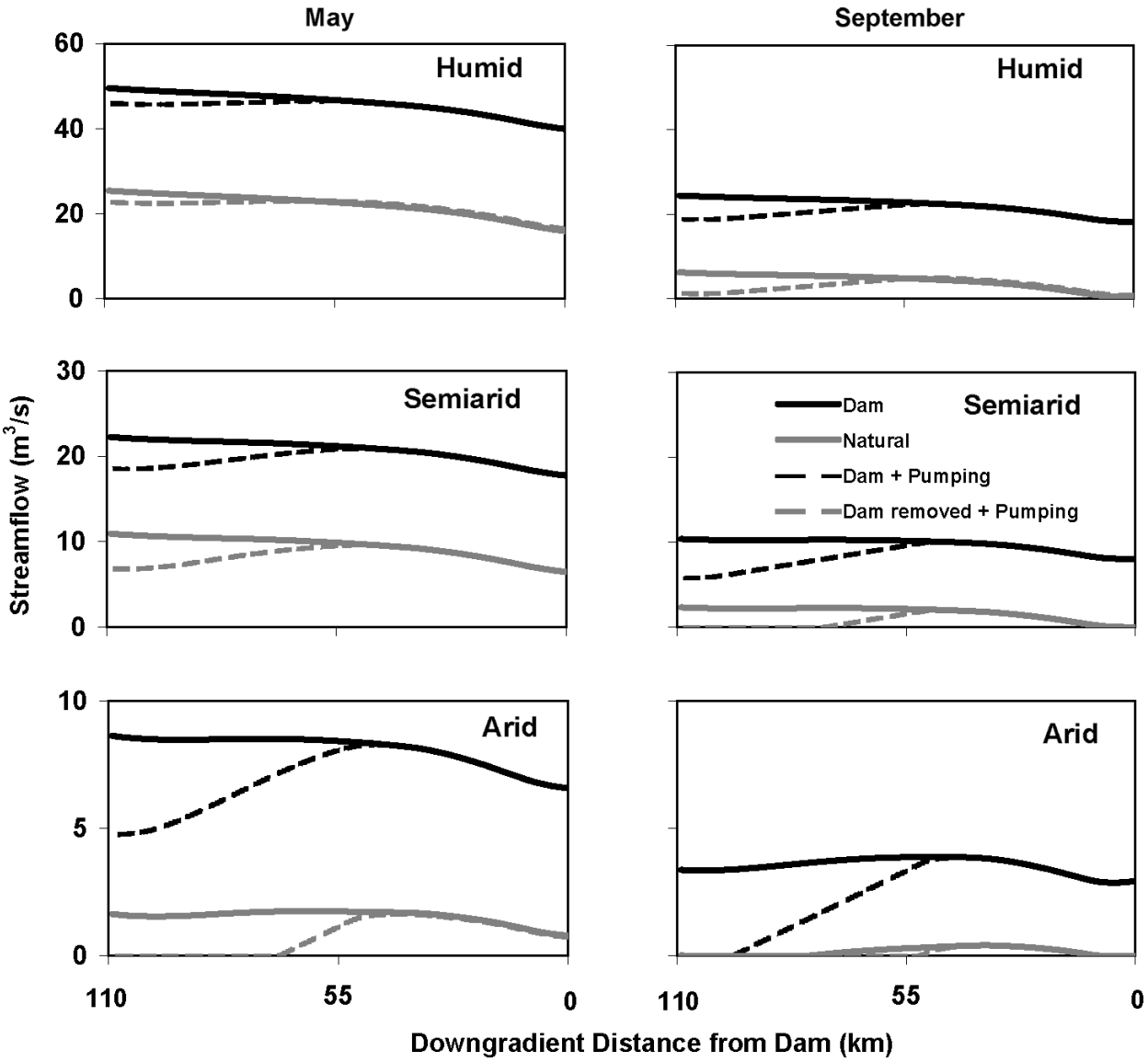

Figure 7. Model-predicted extent of streamflow below the dam site for natural, dam, dam plus pumping, and post-dam and pumping scenarios under humid, semi-arid, and arid conditions in May and September (Note that the outlet of the watershed is located 110 km below the dam site)

and the recovery time to natural streamflow and groundwater conditions may be of interest in the planning stage. Briefly, we addressed this issue by examining the response of streamflow in the humid, semi-arid, and arid watersheds following cessation of pumping using the simulation results from the dam removed with pumping case (Figure 6) as the initial condition. Simulations were run for 2 years beyond scenario 4, by switching off the groundwater extraction option in MODFLOW-2000. We assumed negligible hysteretic behaviour in hydraulic properties and no permanent property changes due to groundwater pumping (e.g. consolidation). Analysis of these simulations indicates that the time required to restore natural groundwater discharge to the stream is a function of climate. For example, 2 years after cessation of pumping, the spatially averaged watershed groundwater discharge to the stream is predicted to recover to 95%, 89%, and 61% of the natural spatially averaged streamflow for the humid, semi-arid, and arid cases respectively. The more gradual recovery with increasing aridity is due to both the greater drawdown due to extended pumping in the drier groundwater basins and to the smaller amount of water available each year to replenish the groundwater system.

CONCLUSIONS

The potential for streamflow restoration following upstream dam removal is impacted by continued groundwater withdrawals, for the range of climatic conditions investigated. Comparative and simulation analyses suggest that, following upstream dam removal, some previously perennial reaches of stream channels might develop ephemeral streamflow in late summer because of continued groundwater pumping and/or the natural conditions of the stream. This transition from perennial to ephemeral flow could have unanticipated impacts on spatial and temporal patterns of streamflow, habitats,

Published in 2006 by John Wiley & Sons, Ltd.

DOI: 10.1002/hyp

and recreational opportunities. Qualitatively, comparative results support the predictions suggested by Constantz (2003) that groundwater pumping will influence post-dam removal streamflow, especially during the low-flow season. Quantitatively, simulation results are consistent with inter-watershed streamflow comparisons regarding the impact of dam removal on streamflow. Inclusion of antecedent groundwater conditions and dynamic groundwater conditions are necessary to predict groundwater exchanges with surface water quantitatively. The novel scheme of generating streamflow from MODFLOW-2000 using the SFR1 packages has clear potential for determining the influence of groundwater on streamflow. This modelling approach has provided a quantitative illustration of the impacts of groundwater pumping on the potential for streamflow restoration, based on four generic scenarios analysed over the long term, monthly to yearly time-frame. As a general conclusion for developed groundwater basins, the most critical impact of dam removal may occur during low flow, when groundwater conditions are most likely to create accelerated reductions in streamflow with associated degradation in the quality of the remaining streamflow.

REFERENCES

Bertoldi GL, Johnston RH, Evenson KD. 1991. Ground water in the Central Valley, CA—a summary report. *United States, Geological Survey, Professional Papers* **1401-A**.

California Irrigation Management Information System. 1999. *Reference evapotranspiration map*. California Department of Water Resources.

Collier M, Webb RH, Schmidt JC. 1996. *Dams and rivers*. US Geological Survey Circular 1126.

Constantz J. 2003. Dams and downstream ground water. *Hydrologic Processes* **17**: 3533–3535.

Constantz J, Essaid H. 2004. The influence of ground water on stream restoration following dam removal. In *Riparian Ecosystems and Buffers: Multi-Scale Structure, Function, and Management, American Water Resources Association Summer Special Conference Proceedings*, Lowrance R (ed.). CD-ROM.

Francisco E. 2004. Tales of the undammed: removing barriers doesn't automatically restore river health. *Science News* **165**: 235.

Freeze RA, Cherry JA. 1979. *Groundwater*. Prentice-Hall: New Jersey.

Graf WL. 1980. The effect of dam closure on downstream rapids. *Water Resources Research* **16**: 129–136.

Gronberg JM, Dubrovsky NM, Kratzer CR, Domagalski JL, Brown LR, Burow KR. 1998. *Environmental setting of the San Joaquin–Tulare basins, California*. US Geological Survey Water-Resources Investigation Report 97–4205.

Harbaugh AW, Banta ER, Hill MC, McDonald MG. 2000. *MODFLOW-2000, the U.S. Geological Survey modular ground-water model—user guide to modularization concepts and the ground-water flow process*. US Geological Survey Open-File Report 00–92.

Kirchner JW, Feng X, Neal C. 2000. Fractal stream chemistry and its implications for contaminant transport in catchments. *Nature* **403**: 524–526.

Landers J. 2004. River renaissance. *Civil Engineering* **74**: (July): 52–59.

Ligon FK, Dietrich WE, Trush WJ. 1995. Downstream ecological effects of dams. *Bioscience* **45**: 183–192.

Manning CE, Ingebritsen SE. 1999. Permeability of the continental crust: implications of geothermal data and metamorphic systems. *Reviews in Geophysics* **37**: 127–150.

Martin G. 2004. Battle of Battle Creek: which way to save salmon? *San Francisco Chronicle* **15**: (March): A1.

McCool D. 2004. As dams fall, a chance for redemption. *High Country News* **21**: (June): 12–13.

National Oceanic and Atmospheric Administration. 2002. *Climatography of the United States No. 81, monthly station normals of temperature, precipitation and heating and cooling days 1971–2000, California*. National Climatic Data Center, Asheville, NC; 73.

Petroski H. 2003. St. Francis dam. *American Scientist* **91**: (March–April): 114–118.

Pohl MM. 2003. Bringing down our dams: trends in American dam removal rationales. *Journal of the American Water Resources Association* **38**: 1511–1520.

Prudic DE, Konikow LF, Banta ER. 2004. *A streamflow routing package (SFR1) to simulate stream-aquifer interaction with MODFLOW-2000*. US Geological Survey Open-File Report 04–1042.

Shuman JR. 1995. Environmental considerations for assessing dam removal alternatives for river restoration. *Regulated Rivers: Research and Management* **11**: 249–261.

Thomas HH. 1976. *The Engineering of Large Dams*. Wiley: London.

Uhlenbrook S, Frey M, Leibundgut C, Maloszewski P. 2002. Hydrograph separations in a mesoscale mountainous basin at event and seasonal timescales. *Water Resources Research* **38**: 31·1–31·14.

Williams GP, Wolman MG. 1984. The downstream effects of dams on alluvial rivers. *United States, Geological Survey, Professional Papers* **1286**.

Winston RB. 2000. *Graphical user interface for MODFLOW, version 4*. US Geological Survey Open-File Report 00–315.